MAGNETOHYDRODYNAMICS Vol. 48 (2012), No. 3, pp. 567–580

CHARACTERISTICS OF ELECTROMAGNETIC INDUCTION BY MOVING FERROFLUIDS

Ching-Yao Chen, Sheng-Yan Wang, Chi-Ming Wu, Chung-Hao Lin, Kuo-An Huang*

Department of Mechanical Engineering, National Chiao Tung University, Hsinchu, Taiwan R. O. C.

We have demonstrated the capabilities to catch the signals of induced electromotive force (EMF). The characteristics of EMF signals are analyzed systematically. Influences of volumes, sizes and travelling velocities of ferrofluids on the magnitudes and wave spans of the signals are presented. In addition, simulations of the induction fields are carried out to provide the physical insights of the induced EMF signals. The signals can be potentially applied as diagnostic characteristics in the measurements of travelling velocities or sizes of moving ferrofluid drops or slugs.

1. Introduction and experimental setup. Magnetorheological (MR) suspension is an artificial and smart fluid consisting of paramagnetic solid particles suspended in a nonmagnetic solvent. A remarkable class of this smart material is the ferrofluid [1], whose particles are nanometer-sized and coated by surfactants. Applications of ferrofluids in multi-stage rotary seals, inertial dampers and loudspeakers had been well-established in the industry [1]. New applications are implemented in the domain of micro-technology as reported in a recent review by Nguyen [2]. In addition, due to its visual appeal and prompt response to magnetic stimuli, this fluid material has become an archetypal dipolar system for the study of a number of pattern-forming processes in engineering and science, i.e. recent progresses in a perpendicular field [3–5] and a radial field [6, 7].

According to the Faraday law, it is also well understood that the induced electromotive force is generated by an unsteady motion of magnetized materials. Devices for measuring the concentration and dispersion quality of magnetic particles by the induced electromotive force had been suggested several decades ago [8]. Electromotive forces induced by ferrofluid motion had also been studied both experimentally and theoretically [9], as well as the reverse situation of liquid motion driven by the thermoelectric current and magnetic field interaction [10]. In recent years, new techniques have been proposed to measure the void fractions and velocities of bubbles in the gas-liquid (ferrofluids) flow system by their electromagnetic induction [11–13]. In addition, understandings of the electromagnetic induction characteristics are also crucial if an electricity conversion device from the moving magnetic fluids is desired [14, 15].

The induced electromotive force (denoted as EMF thereafter) can be obtained by the Faraday law as

$$\mathrm{EMF} = -N\frac{\mathrm{d}\phi}{\mathrm{d}t}, \tag{1}$$

$$\phi = \int (\mathbf{B}\cdot\mathbf{n})\mathrm{d}A, \tag{2}$$

where notations of N, ϕ, and t are the number of identical turns of an induction

* Corresponding author e-mail address: chingyao@mail.nctu.edu.tw

coil, magnetic flux, and time, respectively. **n** and A represent a unit normal vector and the area.

The magnetic induction field **B** can be further expressed by

$$\mathbf{B} = \mu_0(\mathbf{H} + \mathbf{M}), \tag{3}$$

in which μ_0, **H** and **M** are the permeability of vacuum, the magnetic field strength, and the magnetization of ferrofluids, respectively. It is apparent that both the temporal variations of the magnetic induced field and the effective area, which is perpendicular to the magnetic flux, are able to generate the EMF.

In this work, we study experimentally and numerically the characteristics of electromagnetic induction when magnetized ferrofluids pass through the gap of a pair of induction coils. We focus on the influences of relevant physical conditions, such as velocities and sizes of ferrofluids, on the corresponding EMF signals. The results are expected to provide fundamental understandings of the electromagnetic induction of ferrofluids for further applications or studies in more practical or complex conditions.

The experimental setup, as depicted in Fig. 1, consists of a plastic cylindrical container and pairs of induction coils and excitation coils. The cylindrical container, whose diameter is denoted as d_c, is filled with ferrofluids of volume V_0. The corresponding height of the ferrofluids in the container is denoted as h. The ferrofluids are pulled upward by a programmable motor with a constant velocity U to travel through the gap between coils. Detailed layouts of the coils are shown in Fig. 2. The outer diameters of the excitation and induction coils are $L_{EC} = 140\,\text{mm}$ and $L_{IC} = 78.5\,\text{mm}$, respectively. The pairs of coils are placed coaxially with a gap width of $G_{EC} = 130\,\text{mm}$ between the excitation coils. The diameters of coils' central holes are $D_{EC} = 30\,\text{mm}$ and D_{IC} =20.5 mm for the

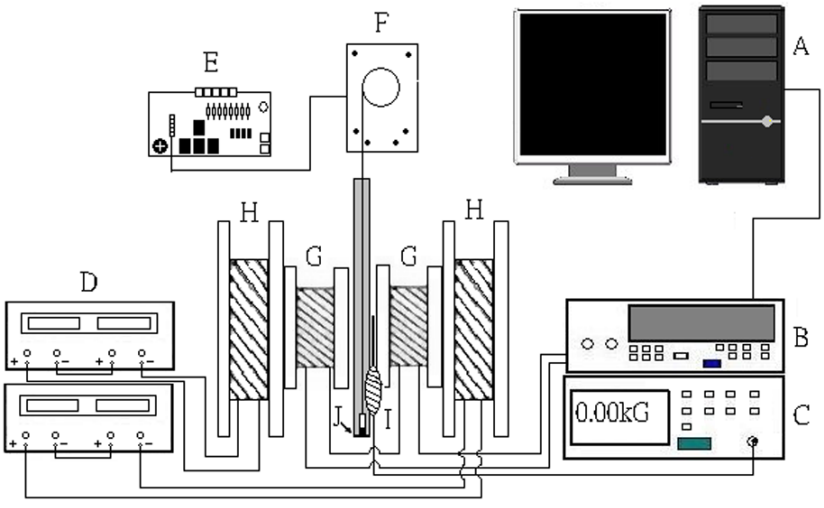

Fig. 1. Principle sketch of the experimental setup: the experimental setup consists of ferrofluids in a cylindrical container (J) magnetized by a pair of excitation coils (H) powered by DC power suppliers (D) and pulled upward by a programmable motor (E and F) to pass through the gap between a pair of induction coils (G).The induction magnetic flux is measured by a probe (I) connected with Gaussmeter (C). The measurements of magnetic flux density and induced electromotive force are recorded by a data logger (B) and transmitted to a personal computer (A) for further analysis.

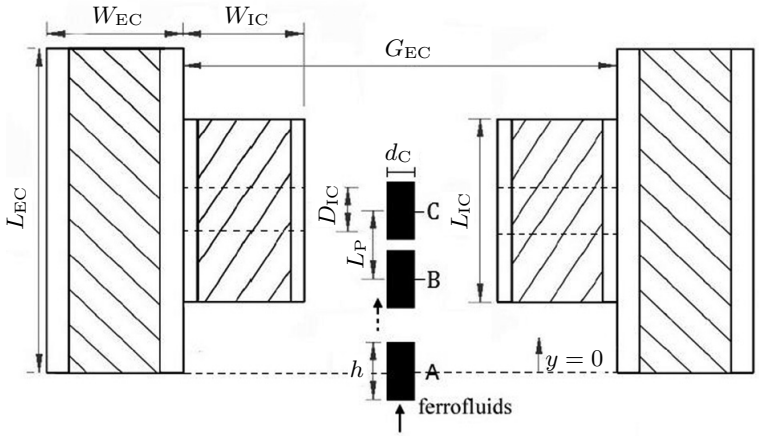

Fig. 2. Layouts of the coils and some important positions of the ferrofluids: positions A and C represent the center of the ferrofluids' mass at the lower edge and at the center of excitation coils, respectively. Position B stands for the location of the ferrofluids, where a maximum magnitude of EMF is induced. The vertical axis $y = 0$ is set at position A.

excitation and induction coils, respectively. The widths of the excitation and induction coils are $W_{EC} = W_{IC} = 58.2$ mm. Each induction coil contains 1500 turns of 0.6 mm-diameter wire. A few important positions are also marked in Fig. 2. Position A representing the center of mass of the ferrofluids is located at the lower edge of the excitation coils and set as the starting position of the vertical axis, i.e. $y = 0$. Position B is where a maximum EMF is induced, and position C is the position at the center of the coils. The ferrofluids used in the experiments are commercial light mineral oil based ferrofluids (EMG905) produced by the Ferrotec Corp. The excitation coils are arranged in a Helmholtz configuration and powered by DC power suppliers, which is somehow different from the earlier experiments [11–13], whose power was supplied by AC sources. A Gaussmeter probe is placed at the center of the coils to record the local magnetic flux density at the centre of the coils. The measurements of magnetic flux density and induced EMF are recorded by a data logger and transmitted directly to a personal computer for further analysis.

2. Results and discussion.

2.1. A representative case. The results of a representative case for ferrofluids with a volume of $V_0 = 4$ ml in a cylindrical container, whose base diameter is $d_c = 12$ mm, moving at a constantly upward velocity of $U = 0.04$ m/s, are first presented. The corresponding height of ferrofluids in such a container is $h = 35.36$ mm. Fig. 3*a* demonstrates the evolution of the originally measured signal of induction magnetic field B at the center of the coils. It is noticed that the initial time $t = 0$ is taken when the ferrofluids' center of mass has reached the bottom edge of the exciting coils (position A shown in Fig. 2). In addition, the signal is truncated when the ferrofluids' center of mass has reached the upper edge. Even disturbed by high-frequency background noises, an apparent bell-shape curve can be clearly identified when the ferrofluids move through the gap of the induction coils. To eliminate the natural noises, high-frequency components are filtered out by the Fast-Fourier-Transform (FFT) technology, and the smoothed signal is also illustrated in Fig. 3*a*. The main features of the signal are well preserved with-

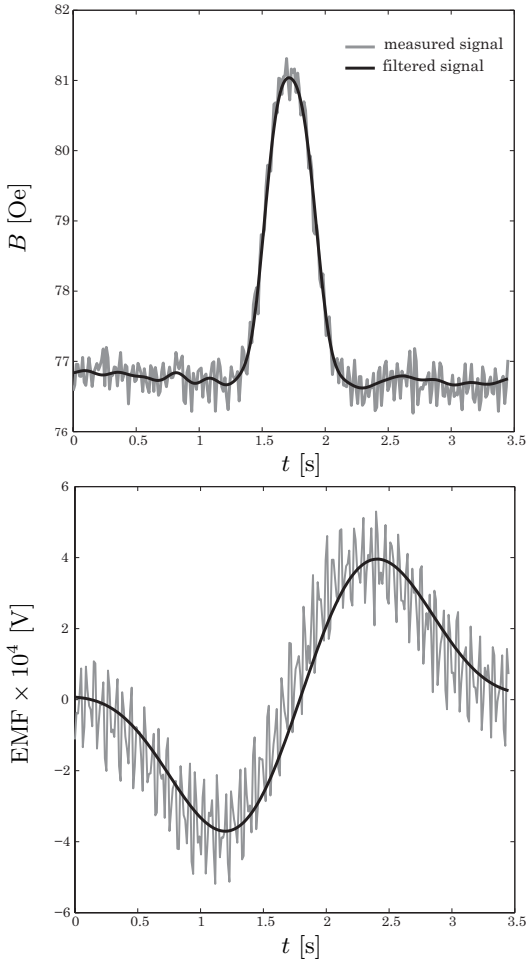

Fig. 3. (*a*) The original and FFT-filtered signals of magnetic flux density recorded by the Gaussmeter placed at the center of coils, and (*b*) the induced EMF signals of the ferrofluids with the volume $V_0 = 4\,\mathrm{ml}$ travelling at a constant upward velocity of $U = 0.04\,\mathrm{m/s}$. The main features of the original signals are well preserved after filtrations of high frequent noises. When the ferrofluids approach the induction coils, the magnetic flux increases and generates the EMF.

out altering their main characteristic, such as the maximum amplitudes and the span of the bell-shape curve. As expressed in Eq. (3), the induction field B is the summation of the applied field H and magnetization M. At the early time stage, when the ferrofluids are still far away from the Gaussmeter located at the central point, the enhancement of the induction field by ferrofluid magnetization is insignificant. The strength of the induction field is almost identical to the external field strength provided by the excitation coils, i.e. $B \approx H \approx 77$ Oe. When the ferrofluids move closer to the coils and are magnetized more significantly, the induction field strength shows a rapid growth. The local induction field strength reaches its maximum magnitude of $B \approx 81$ Oe when the ferrofluids reach the position of the Gaussmeter probe (position C shown in Fig. 2). By the same token, the induction field strength decays significantly when the ferrofluids move continuously away from the centre of the coils and eventually remains at the magnitude of

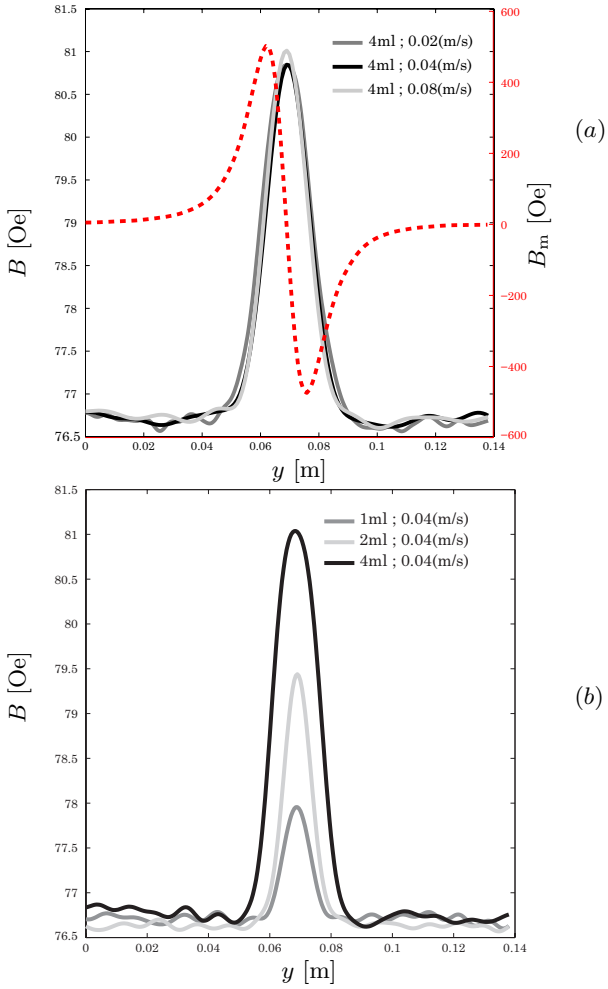

Fig. 4. (*a*) Signals of the magnetic flux density from a permanent magnet (marked by dash line and magnitude indicated at the right axis) and ferrofluids travelling at different velocities, and (*b*) signals of the magnetic flux density by ferrofluids of different volumes. If plotted versus the positions of ferrofluids, the main characteristic features of the local magnetic field depend on their volumes, not travelling velocities.

external field. The dramatic variation of the induction field clearly demonstrates the capability to generate an evident EMF. Nevertheless, the rapid growth and decay of magnetic flux density indicate that the magnetization of ferrofluids is limited within their vicinity.

It is also interesting to note the different characteristics of signals by ferrofluids and by a permanent magnet as shown in Fig. 4*a*. For cases of ferrofluids, whose signals are measured at various travelling velocities $U = 0.02$, 0.04 and 0.08 m/s, their overall shapes remain nearly unchanged if plotted versus their positions of center of mass instead times. It indicates that the maximum magnitudes of the induction magnetic field are independent on the travelling velocities, which meet the general expectations. More detailed discussion regarding the influences of volumes and travelling velocities of ferrofluids will be presented in the next section. On the other hand, an apparent distinction is observed from the signal resulted from a permanent magnet moving with $U = 0.08$ m/s. The induced magnetization

of ferrofluids always aligns along the same orientation of the exciting field, so that the induced field possesses a positive magnitude throughout the entire process and a signal of Gaussian wave is formed. On the contrary, the pole alignment of permanent magnet is predetermined. Consequently, the sign of the magnetic field appears oppositely before and after its pass over the Gaussmeter and results in a sinusoidal signal.

The corresponding measured EMF signals of the representative case before and after the FFT filtration are illustrated in Fig. 3*b*. Again, the main features of the signals are not altered significantly after filtration, so that the filtered signal will be used for the further analysis in the following presentation. As shown in Fig. 3*b*, the EMF signal appears as a sinusoidal wave with the maximum amplitudes EMF $= -3.71 \times 10^{-4}$ V and 3.96×10^{-4} V at times about $t = 1.2$ s and 2.4 s, respectively. The sinusoidal signal can be understood from the Faraday law of Eq. (1), which states the EMF is induced by the negative rate of the induction field. As the corresponding signal of the induction field shown in Fig. 3*a*, when the ferrofluids approach the induction coils, the magnetic flux increases with time and results in the generation of a negative EMF. The increasing rate of magnetic flux density reaches its maximum at the inflection point, whose EMF magnitude also reaches a maximum. After passing over the inflection point, the magnitude of the EMF starts to decay and vanishes at the centre of the coils. This agrees well with the Faraday law that no EMF is induced because of $\mathrm{d}B/\mathrm{d}t = 0$ at this critical position. When the ferrofluids continue their upward travelling into the upper half of the induced coils, the magnetic flux density starts to decline and generates a positive EMF. In addition, the duration of the signal agrees closely with the travelling time of the ferrofluids through the length of the exciting coil at the present velocity, i.e. $L_{\mathrm{EC}} = 138.2$ mm by $U = 0.04$ m/s.

To summarize this section, we have successfully demonstrated the accessibility to generate a sensible induced EMF by a simple DC system. The consistence between the signals of magnetic flux density and induced EMF verifies the capability as well as correctness of our experimental measurements. These typical features of the verified signals, such as their shapes and magnitudes, can be potentially applied as diagnostic characteristics in the measurements of the travelling velocities or sizes of a moving drop or slug of ferrofluids.

2.2. Influences of travelling velocities, volumes and dimensions of ferrofluids. It is understandable that the signals of magnetic flux induced by ferrofluids with a different travelling velocity or volume possess different magnitudes as well as wavelengths. Fig. 4 demonstrates the signals of magnetic flux density measured at the central point versus the positions of the mass center of ferrofluids with various velocities (Fig. 4*a*) and volumes (Fig. 4*b*) in the same container of $d_{\mathrm{c}} = 12$ mm. While the shapes remain almost unchanged for different travelling velocities, as also mentioned in the previous section, a stronger magnetic field results from a larger volume of ferrofluids, as expected. As a result, characteristic features of the induced EMF signals, which are mainly determined by the local variations of the magnetic field, would also depend on the conditions of the ferrofluids. In this section, the influences of these parameters will be discussed.

Fig. 5 shows evolutions of corresponding induced EMF signals at different travelling velocities $U = 0.02$ m/s, 0.04 m/s and 0.08 m/s, respectively, for a fixed volume of $V_0 = 2$ ml (or $h = 17.68$ mm and $d_{\mathrm{c}} = 12$ mm). Apparent distinctions regarding the velocities and amplitudes of the signals can be observed. A faster wave velocity of the EMF signal associated with a larger amplitude is always induced for ferrofluids travelling at a higher velocity. As described in the previous section, the EMF is induced effectively only when the ferrofluids are travelling

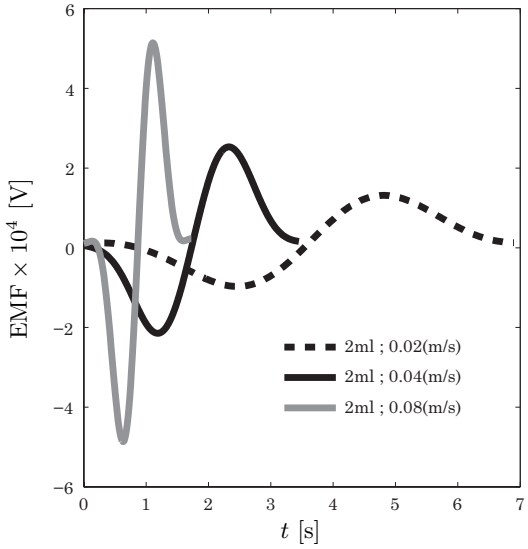

Fig. 5. Induced EMF signals of ferrofluids with different travelling velocities: ferrofluids travelling at a higher velocity always induce EMF signals of faster wave speeds and larger amplitudes.

within the gap of exciting coils. As a result, the time spans (or the wavelengths) of the EMF signals are inversely proportional to the travelling velocities U. The EMF amplitudes, taken as the mean of the lowest negative and the highest positive values, are EMF $= 1.14\times10^{-4}$ V, 2.34×10^{-4} V and 5.01×10^{-4} V for $U = 0.02$ m/s, 0.04 m/s and 0.08 m/s, respectively. It is apparent that a nearly linear relationship is well followed between the travelling velocities and the EMF magnitudes, which can be easily understood from the Faraday law. So, it can be confirmed that the moving velocities of ferrofluids can be effectively determined by the time span of EMF signals decoupled from their magnitudes in the present configuration. Nevertheless, it is usually hard to accurately define the times when the signal exactly starts and vanishes completely. In addition, the actual travelling distance of ferrofluids within the time span of the signal would also be affected by their finite height h rather than the diameter of an excitation coil L_{EC}. A more practical way to determine the travelling velocities of ferrofluids is proposed in the next paragraph.

On the contrary to the ambiguity in defining the time span of the whole signal, the time interval between the peaks of the signal, denoted as t_{p}, can be accurately obtained, such as $t_{\mathrm{p}} = 2.36$ s, 1.19 s and 0.51 s for $U = 0.02$ m/s, 0.04 m/s and 0.08 m/s, respectively, as shown in Fig. 5. The corresponding distances of the peaks from the central point, denoted as L_{p}, as shown in Fig. 2, can be expressed as $L_{\mathrm{p}} = Ut_{\mathrm{p}}/2$. After numerous experiments under various conditions, the positions of peaks are found to remain nearly unchanged for a certain coil configuration regardless of the travelling velocities or volumes of the ferrofluids as $L_{\mathrm{p}} = 24\pm1$ mm in the present setup, as shown in Figs. 5, 6 and 7. It is also interesting to note that this location is very close to the central position of actual thickness of the induction coil, i.e. $L_{\mathrm{p}} \approx (L_{\mathrm{IC}} + D_{\mathrm{IC}})/4$. As a result, the travelling velocities of the ferrofluids can be effectively estimated by $U = 2L_{\mathrm{p}}/t_{\mathrm{p}}$ when the nearly constant value of L_{p} is calibrated by the coil configurations and t_{p} obtained from the EMF signals.

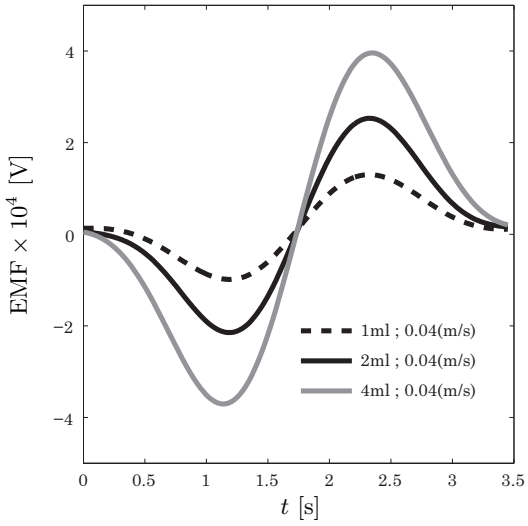

Fig. 6. Induced EMF signals of ferrofluids in various volumes: though higher EMF magnitudes are induced for larger volumes of ferrofluids, a linear proportionality is not necessarily followed in the present experimental conditions.

The volumes of ferrofluids also affect the magnitudes of EMF signals significantly. Shown in Fig. 6, the magnitudes of EMF signals are measured as EMF $= 1.15\times10^{-4}$ V, 2.34×10^{-4} V and 3.83×10^{-4} V for the volumes of $V_0 = 1$ ml ($h = 8.83$ mm), 2 ml ($h = 17.68$ mm) and 4 ml ($h = 35.36$ mm), respectively, at the constant moving velocity $U = 0.04$ m/s. It is worth to emphasize that though a higher EMF magnitude is obtained for a larger volume of the ferrofluids, no linear proportionality is followed, which is somehow out of initial expectation. This unexpected result is mainly attributed by the size (or shape) effects of the ferrofluids. Though full understandings of these size effects have to rely on the complete distributions of induced magnetic fields, one apparent factor can be easily addressed. It is reasonable that the induced EMF is directly proportional to the magnetization strength within the effective area. Nevertheless, since the hollow induction coil contains a central hole as shown in Fig. 2, the actual thickness of the coils is $(L_{\mathrm{IC}} - D_{\mathrm{IC}})/2 = 29$ mm. For the above cases of $V_0 = 1$ ml, 2 ml and 4 ml, whose heights are, respectively, $h = 8.83$ mm, 17.68 mm and 35.36 mm, it is apparent that only the first two cases can be fully covered by the coils. It gives a partial explanation why the increments of EMF magnitudes appear nearly linear for the first two cases, but smaller when the volumes of the ferrofluids become too large. A relevant issue of the size and shape effects can also be confirmed by experiments with the same ferrofluids volumes in containers with different base areas. Fig. 7 shows the results for the case of $V_0 = 2$ ml and $U = 0.04$ m/s in containers with different base areas. The heights of ferrofluids are $h = 16.56$ mm, 15.57 mm, 10.76 mm and 6.30 mm, and their corresponding induced EMF magnitudes are measured as EMF $= 2.63\times10^{-4}$ V, 2.78×10^{-4} V, 2.95×10^{-4} V and 3.29×10^{-4} V, respectively. Small but apparent variations are observed, in which higher EMF magnitudes are induced for the cases with lower heights. It is clear that ferrofluids with a lower height concentrate the induced magnetic flux more effectively so that a stronger EMF is generated. More detailed discussion regarding this issue will be presented in the following section of numerical simulations.

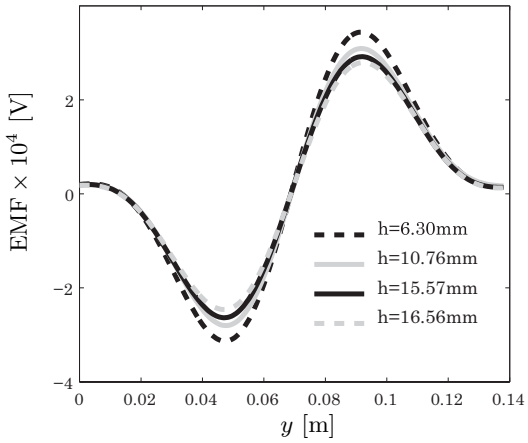

Fig. 7. Induced EMF signals of ferrofluids with a constant travelling velocity of $U = 0.04\,\mathrm{m/s}$ and a volume of $V_0 = 2\,\mathrm{ml}$ in containers of different base sizes: insignificant but distinguishable higher EMF magnitudes are induced for the cases with lower heights.

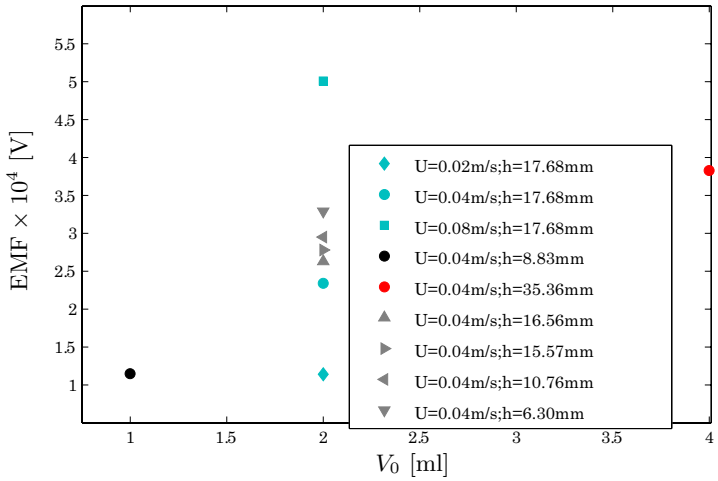

Fig. 8. Mean magnitudes of the maximum induced EMF for various experimental conditions.

A final point to be stressed is that these dimensional effects of ferrofluids can be potentially applied to distinguish the size of a ferrofluid drop or slug.

Numerous experiments were conducted by applying several magnetic field strengths to ferrofluids with various travelling velocities in containers of different sizes, as their corresponding EMF values are demonstrated in Fig. 8. A very consistent qualitative trend is confirmed and thus the results presented above are valid robustly. Based on the results discussed, it can be summarized that the features of the induced EMF signals are affected mainly by three characteristics of ferrofluids, such as travelling velocities, volumes and dimensions. In the other words, these characteristics of ferrofluids can be effectively estimated if their correlations with the shapes and magnitudes of the measured signals are well established for a particular coil configuration. This provides an alternative technology of flow measurements.

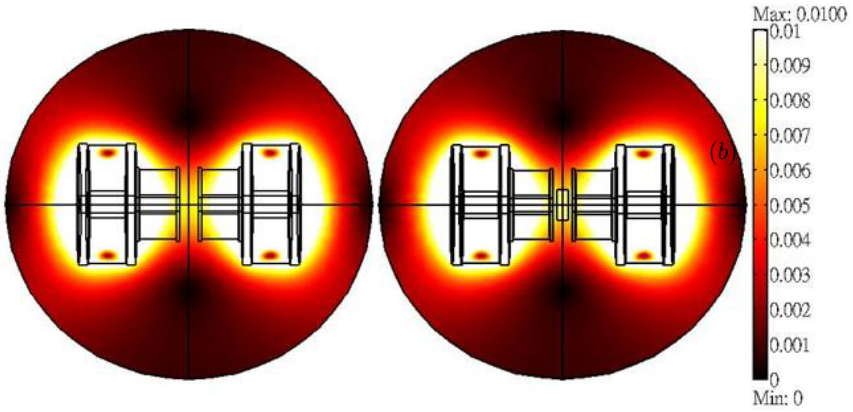

Fig. 9. Numerical simulations of induction field distributions in the middle cross-section: (a) without ferrofluids, (b) with ferrofluids with $V_0 = 4\,\mathrm{ml}$ at position C.

2.3. Numerical simulations of induced magnetic fields. As mentioned in the previous section, the effects of sizes and dimensions of ferrofluids on the induced EMF cannot be understood completely without detailed realizations of their corresponding magnetic fields. In this section, the induced magnetic fields governed by the Maxwell equations are numerically simulated in terms of the magnetic vector potential $\mathbf{A}$ written as

$$\mathbf{B} = \nabla \times \mathbf{A}, \tag{4}$$

$$\nabla \times \left(\frac{1}{\mu_0} \nabla \times \mathbf{A} - \mathbf{M} \right) = \mathbf{J}. \tag{5}$$

$\mathbf{M}$ is the magnetization of ferrofluids, and $\mathbf{J}$ is the current density. The magnetization is taken as $M = C_1 \tan^{-1}(C_2 H)$, whose constants $C_1 = 10^4$ and $C_2 = 3 \times 10^{-5}$ are obtained by curve-fitting with the actual measurements. The set of full 3D equations is solved by the commercial available COMSOL Multiphyscis package. Shown in Fig. 9 are the detailed magnetic fields of tested cases without and with ferrofluids present at the center of coils (position C in Fig. 2) in the middle cross-section, which indicate the local enhancement of the induction field strength by the presence of the ferrofluids. To further demonstrate the induction enhancement more clearly, contours of the induction field in a 2D pattern are displayed in Fig. 10. The field contours are seen to accumulate at the edges of the ferrofluids and result in stronger strengths locally. The local accumulations are attributed by sudden variations of the magnetization within the ferrofluids and air. To validate this localization of the induction field, comparisons between the simulations illustrated in Fig. 9 and the actual measurements of field strengths along the vertical middle line are made (Fig. 11). An excellent agreement is obtained for the case without ferrofluids, whose field increases gradually and reaches the maximum at the center of the coils. For the case with the ferrofluids, the region occupied by the ferrofluids cannot be measured by a Guassmeter, so that the measurements are available only right outside the container. A fair agreement is obtained within the region, where measurements are available. Most importantly, an apparent dip of the field strength right outside the edge of the ferrofluids is both observed by measurement and simulation, which validates the correctness of the simulation to catch such a rapid change. The dip associated with the sudden bump immediate

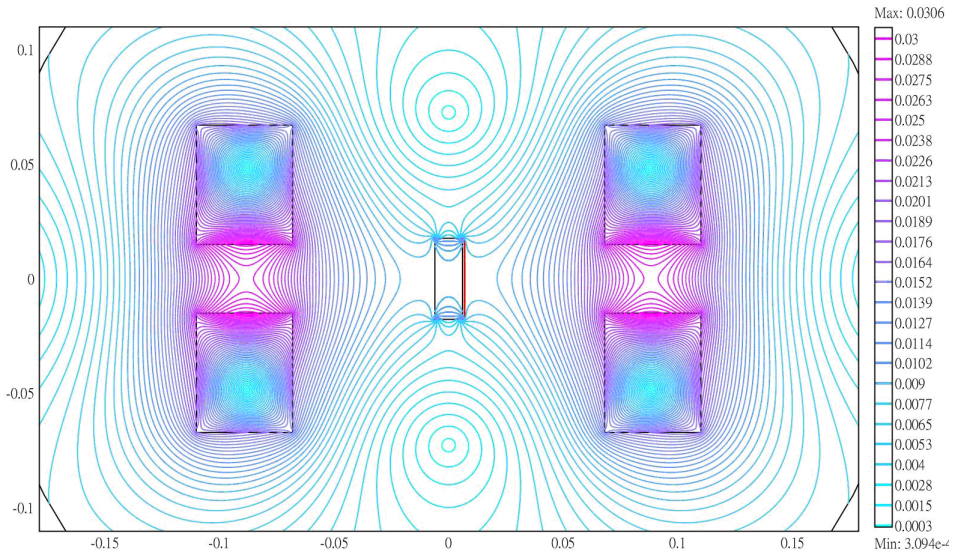

Fig. 10. Typical pattern (2D pattern) of induction field contours by the presence of ferrofluids at position C. Field contours local accumulation at the upper and lower edges of the ferrofluids is clearly observed.

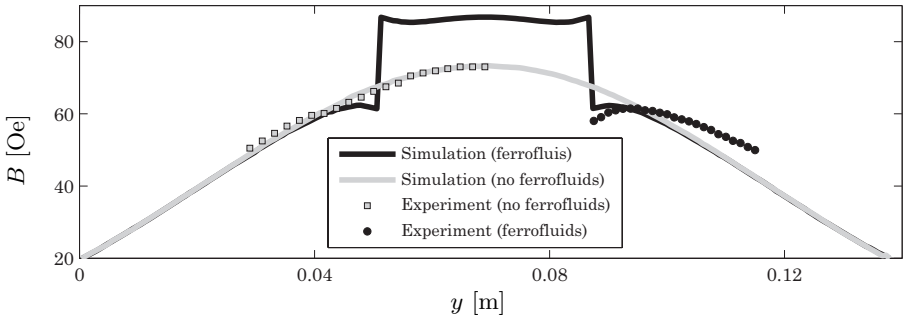

Fig. 11. Induction field distributions along the middle line for the cases shown in Fig. 9. Reasonable agreements are obtained between the available experimental measurements and the numerical results.

within the ferrofluids demonstrates the localization of magnetic flux contours. In addition, enhancement of the magnetic strength appears only within the region occupied by a ferrofluid, which also meets the general expectation. These facts verify the creditability of the simulations.

Simulations of the representative case shown in Fig. 3 are first presented. The induction field strengths along the middle line for various positions of ferrofluids, denoted as y_f, are shown in Fig. 12*a*. Note that the increasing height from $y_\mathrm{f} = 0\,\mathrm{mm}$ to $y_\mathrm{f} = 70\,\mathrm{mm}$ evidences that the ferrofluids are travelling upward from position A to position C shown in Fig. 2, accordingly. Consistent with the results mentioned above, all the profiles collapse exactly with the curve of the background external field except the region occupied by the ferrofluids. The increments of the magnetic flux, which can be represented by the area differences from the curve of the external field, grow as the ferrolfuids move upward and reach the maximum at the central position at $y_\mathrm{f} = 70\,\mathrm{mm}$. The magnetic flux variations

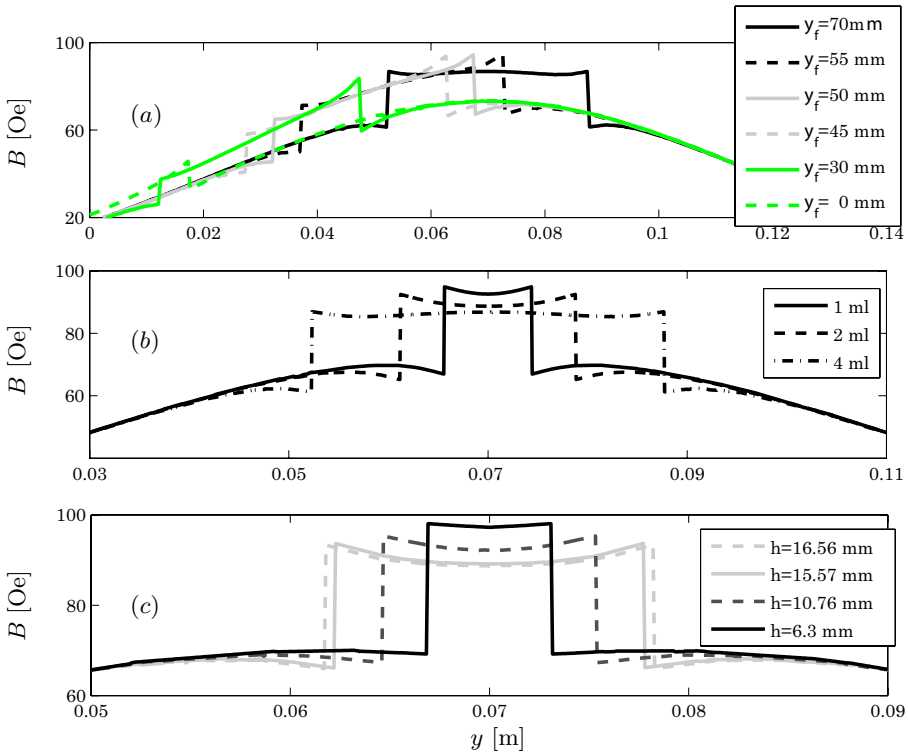

Fig. 12. Induction field distributions along the middle line: (*a*) the case of $V_0 = 4\,\mathrm{ml}$ for various positions of ferroluids (y_f), (*b*) cases of ferrofluids at position C with various volumes, and (*c*) cases of ferrofluids at position C with various heights. Note that $y_\mathrm{f} = 0\,\mathrm{mm}$ and $70\,\mathrm{mm}$ correspond to positions A and C, respectively.

explain why the EMF signal behaves like a sinusoidal wave with zero-magnitude at position C, as shown in Fig. 3*a*. Shown in Fig. 12*b* are the field distributions along the middle line of the ferrofluids with different volumes in containers of identical base area at $y_\mathrm{f} = 70\,\mathrm{mm}$ (position C). Their corresponding EMF signals are shown in Fig. 6. It is interesting to observe that though the overall increment of the magnetic flux is larger for a bigger volume of ferrofluids because of its wider magnetizing width, the maximum magnitude of the induced field strength is found to be stronger for a smaller volume of ferrofluids. This result is caused by the local accumulation of magnetic flux, as demonstrated in Fig. 11. For the case of a less amount of ferrofluids, the magnetized region is shorter. Considering the present configurations of non-uniform external field distribution, the ferrofluids would be exposed in the area of stronger external field strengths. As a result, the local accumulations of the magnetic flux at the edges are more significant and thus lead to a higher magnitude of the induced magnetic field strength. This could be another reason why the total magnetic flux does not follow a linear relation respondent to their volumes of magnetized ferrofluids. Similar results are obtained for the cases of identical volume of ferrofluids in containers with different base areas, as the field distributions shown in Fig. 12*c*. The trend is consistent with the previous cases, such that a stronger local field is induced at a lower height and partially explains a slightly bigger induced EMF magnitude shown in Fig. 7.

3. Concluding remarks. In this paper, we study both experimentally and theoretically the characteristics of electromagnetic induction when magnetized fer-

rofluids pass through a pair of induction coils. Effects of various parameters, such as volumes, dimensions and travelling velocities of ferrofluids, on the magnitudes of the corresponding induced electromotive force (EMF) were investigated. The signals of the induced EMF are enhanced with the increasing volume of the ferrofluids and their travelling velocities, as expected. Nevertheless, the dimensions of the ferrofluids, such as the base areas of containers and the ferrofluid effective heights, also affect the induced EMF signals. Numerical simulations of the induced fields were performed to obtain detailed field distributions and provide useful insights. The signals can be potentially applied as alternatives in the measurements of the flow fields after a detailed correlation and calibration are established.

Acknowledgments. Supports by the National Science Council of the Republic of China under grant NSC 98-2221-E-009-114-MY3 is acknowledged.

REFERENCES

[1] R.E. Rosensweig. Ferrohydrodynamics. (Cambridge University Press, Cambridge, England, 1985).

[2] N.T. Nguyen. Micro-magnetofluidics: Interactions between magnetism and fluid flow on the microscale. *Microfluid Nanofluid*, 12:1-16 (2012).

[3] C.-Y. Chen, W.-K. Tsai, and J.A. Miranda. Experimental study of a hybrid ferrohydrodynamics instability in miscible ferrofluids: droplet size effects. *Magnetohydrodynamics*, vol. 45 (2009), no. 1, p. 3–14.

[4] C.-Y. Chen, C.-S. Li. Ordered microdroplet formations of thin ferrofluid layer breakups. *Phys. Fluids*, 22, 014105 (2010).

[5] C.-Y. Chen, J.-F. Liu, and L.-C. Wang. Instability patterns of ferrofluids immersed in a fluid layer. *Magnetohydrodynamics*, vol. 46 (2010), no. 3, p. 235–244.

[6] C.-Y. Chen, Y.-S. Yang, and J. A. Miranda. Miscible ferrofluid patterns in a radial magnetic field. *Phys. Rev.*, E 80, 016314 (2009).

[7] C.-Y. Chen, W.-L. Wu, and J. A. Miranda. Magnetically induced spreading and pattern selection in thin ferrofluid drops. *Phys. Rev.*, E 82, 056321 (2010).

[8] T.M. Kwon, M.S. Jhon, and T.E. Karis. A device for measuring the concentration and dispersion quality of magnetic particle suspension. *IEEE Transactions on Instrumentation and Measurement*, 41, 1, 10–16 (1992).

[9] A.A. Kubasov. Electrmotive force generation due to ferrofluid motion. *Journal of Magnetism and Magnetic Materials*, 193, 15–19 (1997).

[10] I. Kaldre, Y. Fautrelle, J. Etay, A. Bojarevics and L. Buligins. Investigation of liquid phase motion generated by the thermoelectric current and magnetic field interaction. *Magnetohydrodynamics*, vol. 46 (2010), no. 4, p. 371–380.

[11] S. Shuchi, H. Yamaguchi and M. Takemura. Measurement of void fraction in magnetic fluid using electromagnetic induction. *J. Fluids Eng.*, 125, 479 (2003).

[12] T. Kuwahara and H. Yamaguchi. Void fraction measurement of gas-liquid two-phase flow using magnetic fluid. *J. Thermophys. Heat Transf.*, 21, 173 (2007).

[13] T. Kuwahara, F.De Vuyst, and H. Yamaguchi. Bubble velocity measurement using magnetic fluid and electromagnetic induction. *Phys. Fluids*, 21, 097101 (2009).

[14] F. Gazeau, C. Baravian, J.-C. Bacri, R. Perzynski, and M.I. Shliomis. Magnetic nanoparticles as motors of energy conversion in ferrofluids: generators. *Phys. Rev.*, E 56, 614618 (1997).

[15] S. Carcangiu, A. Montisci and R. Pintus. Performance analysis of an inductive MHD generator. *Magnetohydrodynamics*, vol. 48 (2012), no. 1, p. 115–124.

Received 12.09.2012